Two-Photon Photochemistry of CdSe Quantum Dots

Youhong Zeng and David F. Kelley*

Chemistry and Chemical Biology, University of California Merced, 5200 North Lake Road, Merced, California 95343, United States

ABSTRACT The two-photon photochemistry of CdSe quantum dots (QDs) has been systematically studied. We find that upon intense irradiation CdSe quantum dots that absorb two or more visible photons undergo photodarkening. The quantum yield for this process is on the order of 6% in chloroform and much smaller in nonpolar solvents, such as octane. An analysis of the energetics indicates that, following two-photon excitation, the biexciton undergoes an Auger process producing a hot hole. This hot hole is ejected to a surface-bound TOP ligand, forming a QD^{-}/TOP^{+} contact ion pair that separates in chloroform, but not in octane. The charged and deligated QD is dark, resulting in the overall photodarkening. This photodarkening reaction may or may not be reversible, depending on what other chemical components are in the irradiated solution. The quantum dot concentration dependence and PL decay kinetics indicate that charge recombination occurs rapidly, followed by ligand reattachment and reorganization on a longer (tens of minutes) time scale. The relation of this mechanism to one-photon photochemistry is also discussed.

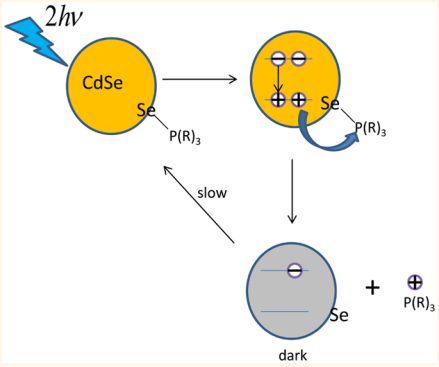

KEYWORDS: quantum dots · photochemistry · two-photon · nanocrystals · photodarkening · ionization · ligands

Intense or extended irradiation often changes the optical properties of CdSe quantum dots (QDs). In many cases, the effect of irradiation is "photoannealing", which increases the photoluminescence (PL) quantum yield (QY).[1−9] In other cases, there is a reversible or irreversible decrease in luminescence intensity.[10,11] The loss of luminescence is usually assigned to nonradiative processes associated with photoinduced particle charging. This is particularly true under conditions of intense irradiation, where there is a significant probability of biexciton or multiexciton formation. Biexciton Auger processes can produce highly excited charge carriers that can be ejected from the particle, and it is believed that particle charging is the primary step in the loss of PL intensity and the subsequent photochemistry.[12−16] This Auger-assisted photoionization has been shown to occur in PbS and PbSe nanocrystals.[17] The subsequent photochemistry has been a significant problem in time-resolved optical studies, which often employ intense photoexcitation, and this has been particularly true for transient absorption studies of multiexcitons.[18−24] Charge ejection can also occur following photoexcitation with photons having energy that is much greater than the bandgap.[25−27] In these cases, photoexcitation directly produces hot carriers, and interfacial charge transfer competes with carrier cooling. Particle charging and ligand reactions can have a dramatic effect on the photoluminescence dynamics. Photoexcitation of a charged particle can produce a positive or negative trion—a species with two holes and one electron or two electrons and one hole. Trions generally have low luminescence QYs due to radiationless decay through an Auger process.[22,28,29] Ligand loss can also produce species with greatly reduced PL QYs. The ligand binding site can act as an electron or hole trap, which facilitates radiationless charge recombination. As a result, PL intensity kinetics can be used as a probe of reaction rates involving charging and/or ligand reactions, and as such, these kinetics can be analyzed to infer the nature of the photochemistry induced by the intense irradiation. Although photoinduced charging or surface chemistry is very common and often dominates the photophysics of quantum dots, to the best of our knowledge, no mechanistic studies of two-photon photodarkening have been reported.

In this paper, we examine the initial step and subsequent mechanism of the two-photon

* Address correspondence to dfkelley@ucmerced.edu.

Received for review July 29, 2015 and accepted September 15, 2015.

Published online September 15, 2015
10.1021/acsnano.5b04710

(biexciton) photochemistry of CdSe QDs. The QDs used in this study are obtained from a very standard synthesis.[30] This synthesis (details given in the Experimental Section) involves the reaction of a cadmium alkyl carboxylate with excess trioctylphosphine selenium in the presence of excess alkylamine and trioctylphosphine oxide. The solvent is octadecene, and the reaction is run at about 260 °C. We examine several sizes of particles and different surface chemistries. We focus on particles having diameters of about 3.4 nm and have somewhat selenium-rich surfaces. Purification is done by polar/nonpolar solvent extraction, which is a standard purification method. The PL quantum yields are typically 20−25%, making this type of QD extremely common. When these particles are dissolved in room-temperature chloroform and briefly subjected to pulses of intense near-UV light, their PL quantum yield is reduced. Depending upon conditions, the quantum yield may or may not subsequently recover. When recovery does occur, it takes place on the tens of minutes time scale. It is the photochemical reactions associated with PL depletion and recovery that we elucidate in this paper. The approach used here is that of classical chemical kinetics: reaction rates are measured as a function of concentrations of different species in solution. Following a brief (several seconds) exposure to intense photoexcitation, samples are exposed to very low intensity excitation, and the intensity of the PL is measured over the course of the next several tens of minutes. These kinetics are obtained with different concentrations of the QDs as well as several other species in the solution, and the results are analyzed to infer the reaction mechanism.

RESULTS AND DISCUSSION

1. Power Density Dependent Photodarkening: A Two-Photon Process. CdSe QDs can undergo photochemistry as a result of either one- or two-photon processes. It is therefore necessary to first establish that the PL depletion observed here is as a result of absorption of two photons, producing a biexciton. The possibility of simultaneous two-photon absorption to produce a highly excited single exciton can also be considered. The cross-sections for two-photon absorption in CdSe QDs have been measured and are on the order of 6×10^4 GM ($1\ \mathrm{GM} = 10^{-50}\ \mathrm{cm}^4\ \mathrm{s\ photon}^{-1}$).[31,32] Using this value and the known extinction coefficients for CdSe,[30,33,34] the ratio of direct two-photon absorption to sequential two photon absorption to produce biexcitons can be calculated. This calculation assumes that the absorption cross section is independent of having absorbed one photon. This is a good assumption because of the high density of states at the excitation energy, 3.2 eV. This calculation reveals that the extent of direct two-photon absorption is 4−5 orders of magnitude lower than sequential biexciton production, which is consistent with the observation that direct two-photon absorption is typically observable only with sub-bandgap excitation. Direct two-photon absorption will not be further considered.

To establish that biexcitons give rise to the observed photodarkening, several identical samples of CdSe QDs were purified by two acetone/hexane precipitations, followed by resuspension in pure chloroform. No other species were added to the solutions, each having a volume of 1.5 mL and a QD concentration of 1.7×10^{-6} M. The rapidly stirred samples are prepared in 1 cm cells and subjected to 10 s of irradiation with a focused beam of 1 kHz, 387 nm, 140 fs pulses. The 1.0 cm diameter beam is focused down with a 50 cm lens with the total power held constant as 18.5 mW. The power density is varied by controlling the position of the samples with respect to the focus. The result is that the number of two-photon absorptions is varied while the total number of photons absorbed remains constant. This is very similar to other "z-scan" methods of determining nonlinear optical properties.[35,36] Immediately following exposure, the sample cells are transferred to take the emission spectra with very low excitation intensity. The resulting PL spectra are shown in Figure 1a. The PL intensity decreases with increasing power density of the irradiation, indicative of a multiphoton process. Under these conditions, the final PL spectra and intensities are stable; *i.e.*, the loss of PL intensity is essentially irreversible.

The extent of reaction (PL loss) varies with sample position and, therefore, with the probability of two-photon excitation. This dependence is shown in Figure 1b and can be modeled using a Poisson distribution to describe the number of photons absorbed by each particle during each laser pulse. The sample is not optically thin, so the beam intensity and hence the probability of two-photon absorption varies with the position in the cell. The probability of a QD in the irradiated volume absorbing two or more photons in a single pulse is given by

$$P_{\geq 2} = \int_0^L \mathrm{d}x \sum_{n\geq 2} P(n; m(x)) \qquad (1)$$

where $P(n;m)$ is a Poisson distribution in the integer variable n having an average of m. The average number of photons absorbed per particle per pulse is given by

$$m(x) = m_0 \exp(-2.303 A_{387} x/L)$$

where A_{387} is the sample absorbance at 387 nm, m_0 is the average at the front of the cell, and x is the position in the cell of length L. The value of m_0 is given by

$$m_0 = \frac{2303 \epsilon_{387} P_{\mathrm{beam}}/1000}{N_{\mathrm{A}}(hc/\lambda)\mathrm{area}}$$

where the laser repetition rate is 1000 (s^{-1}), the area is the irradiation spot size (cm^2), P_{beam} is the incident excitation power (0.0185 W), ε_{387} is the 387 nm extinction coefficient (taken to be 3.3×10^5 L $\mathrm{mol}^{-1}\mathrm{cm}^{-1}$ for

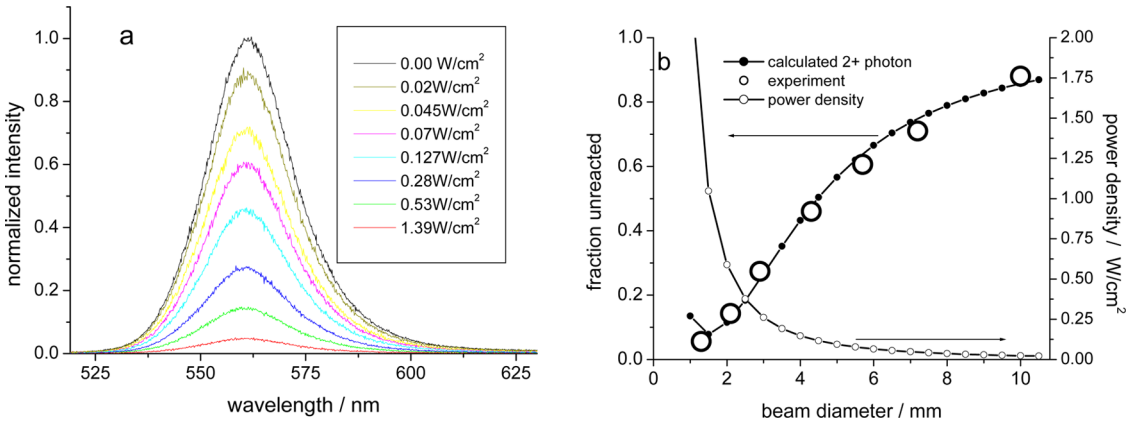

Figure 1. (a) Emission spectra of CdSe after irradiation with different power densities. (b) Filled dotted line is the fraction of unreacted particles plotted versus the diameter of the beam, calculated as described in the text; open circles are experimental results obtained from (a). Also shown are the average total power densities (open dotted line).

these particles[33]), and N_A is Avogadro's number. We note that

$$\frac{P_{beam}/1000}{(hc/\lambda)\text{area}}$$

is the incident photon density (photons pulse^{-1} cm^{-2}) at the front of the cell. In summing over $n \geq 2$, eq 1 assumes that reaction occurs only following absorption of two or more photons. The integral in eq 1 is evaluated numerically to give the fraction of particles in the focal volume that absorb two or more photons. The beam diameter is typically a few millimeters at the sample cell, so the focal volume is a small fraction of the total sample volume. However, because the cell is rapidly stirred, the fraction of reacted particles is spatially homogeneous. With this assumption, the overall reaction probability per pulse, denoted as P_{tot}, is given by the product of $P_{\geq 2}$ and the ratio of the irradiated and total volumes:

$$P_{tot} = P_{\geq 2}\frac{\text{area} \times L}{\text{total volume}}$$

This probability is multiplied by the total number of pulses in the irradiation experiment, *1000*·time (s), and the reaction quantum yield, Φ_{rxn}, to give the average number of reactive events per particle during irradiation. The fraction of unreacted particles is evaluated from a Poisson distribution, with

$$\text{fraction unreacted} = P(0; 1000P_{tot}\Phi_{rxn}\text{time(s)})$$

This approach tacitly assumes that once a two-photon reaction event has occurred subsequent two-photon absorption has no further effect. The validity of this model is assessed by how well the power density dependent results match the observed reaction probability. A plot of the unreacted fraction calculated as a function of beam diameter is shown in Figure 1b. This plot assumes a reaction quantum yield of 0.058, which is the only adjustable parameter in the calculation. Excellent agreement with the experimental measurements is obtained, showing that two or more photons are needed to cause photodarkening. We note that the reaction quantum yield depends on the nature of the QD surface. Specifically, we find that the reaction probability is much lower (about a factor of 5) when the nanocrystal surface is cadmium rich. This indicates that selenium bound ligands are involved in the photodarkening mechanism, as discussed below.

2. Solvent and Ligand Dependence: Hole-Transfer Photoionization. Figure 2A shows that the extent of PL depletion after irradiation depends on the polarity of the solvent. Very little PL depletion occurs in pure octane or in octane with an excess of oleylamine (OAm) and TOP. Thus, independent of the other species in solution, the two-photon photodarkening has a much lower reaction probability in a nonpolar solvent. This observation has a very simple and obvious interpretation: the depletion mechanism involves ionic intermediates and/or ion pair separation.

Figure 2B shows that the extent of PL recovery depends on the presence of other reagents in the chloroform solution. The PL depletion results shown in Figure 1 were obtained with the QDs suspended in pure chloroform and were irreversible; little or no recovery occurs on the minutes to hours time scale. Particles dispersed in chloroform/OAm also show essentially no PL recovery. Very different kinetics are observed in the presence of an excess of an electron donor ligand, such as a trialkylphosphine or triethylamine. An excess of trioctylphosphine (TOP) or tributylphosphine (TBP) results in a slow (tens of minutes) recovery of the PL intensity. The presence of triethylamine (TEA) in the solution results in a similar, but somewhat faster, recovery. It is of interest to note that in the presence of TEA the final PL intensity exceeds the initial value. We note that if these particles are ligand exchanged with TEA the effect is an increase in PL intensity. Taken together, these observations indicate that the depletion/recover process has the effect of exchanging surface ligands with those in solution. Thus, Figure 2 underscores two observations that are

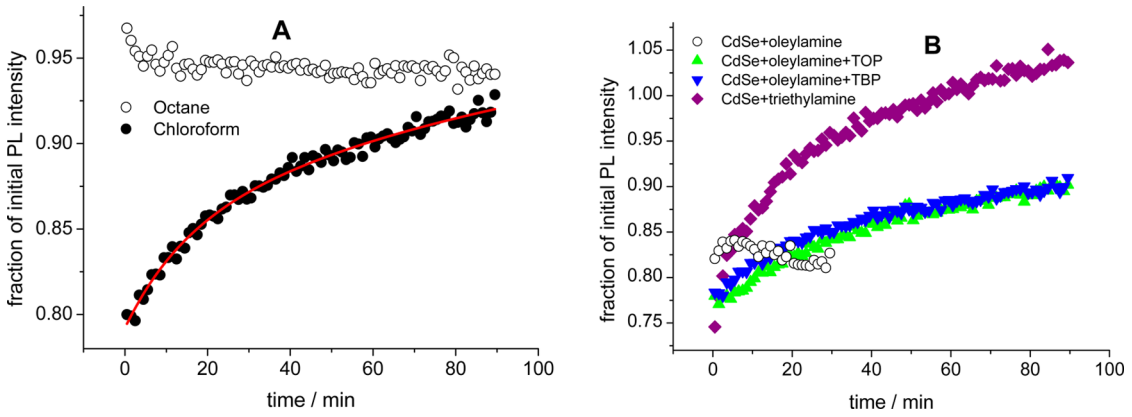

Figure 2. (A) PL recovery kinetics for samples with the same concentration of TOP and oleylamine in chloroform and octane. Also shown is a fit curve corresponding to 15 (30%) and 120 (70%) minute PL recovery components. (B) PL recovery kinetics for samples with different ligands in the chloroform solution.

central to assigning the mechanism of PL loss and recovery: first, that PL depletion occurs only in a polar solvent, and second, that PL recovery occurs only when excess of TOP or a similar Lewis base ligand is present in the solution.

These observations suggest that both ionization and the loss and gain of surface ligands are involved in the overall photochemistry. It is therefore important to establish the time scale on which ligand reactions occur. Figure 3 shows the effect of adding excess ligands to a well-purified QD sample in chloroform with excess OAm. Repeated purification by polar/nonpolar extraction and precipitation removes some fraction of the surface passivation ligands, so the quantum yield is initially fairly low, typically about 10%. Addition of excess ligands (in this case TOP) results in an immediate decrease in the PL intensity, followed by a subsequent recovery. It is important to note that no irradiation is involved in the Figure 3 kinetics; this simply measures the ligation time scale as determined from the PL intensities. The initial PL decrease is likely due to a slight etching of the surface, specifically removal of some of the least tightly bound surface atoms. We suggest that the subsequent recovery of the QY is due to passivation of the newly-formed recombination sites on the particle surface. Figure 3 shows that the PL intensity relaxes to a higher value rapidly at first and then more slowly. It also shows that the rate of PL recovery does not increase with increasing TOP concentration, which is a notable result. One would expect that if the passivation reaction were the simple addition of a TOP to a surface recombination site, then this rate would increase with the solution TOP concentration. However, Figure 3 shows that only the fast component of the recovery is concentration dependent. The concentration independence of the dominant slower component indicates that this reaction corresponds to a process in which TOP addition is not the rate-limiting step. This suggests that subsequent ligand-exchange reactions (presumably with an OAm ligand) are also involved in the PL recovery kinetics. The details of these ligands reactions are beyond the scope of this paper. However, the important point is that the room-temperature ligand addition and exchange reactions take place on the tens of minutes time scale.

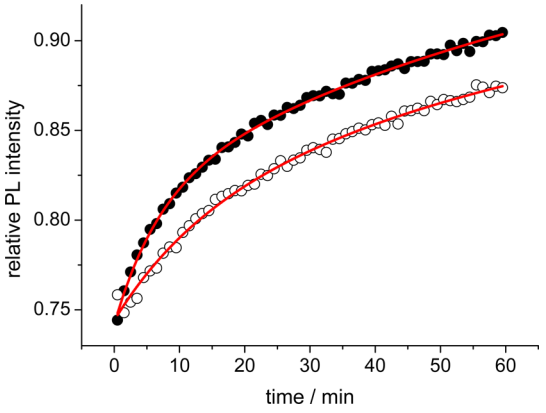

Figure 3. PL increase kinetics following the addition of TOP at a concentration of 16.8 mM (solid circles) or 45 mM (open circles) to a purified sample of QDs dissolved in chloroform and excess (50 mM) oleylamine. Also shown are biexponential fits corresponding to 6.9 (30%) and 80 (70%) minute relaxation components (top curve) and 13.2 (25%) and 80 (75%) minute relaxation components (bottom curve).

The ligation kinetics in Figure 3 are quite similar to the PL recovery kinetics shown in Figure 2; both are dominated by long components of about 100 min. In the case of Figure 3, there was no irradiation, and the only processes that can occur are ligand addition and exchange reactions. The similar rates from these two very different types of experiments suggests that ligand reactions are also the rate-limiting step in the long component of the PL recovery kinetics following irradiation shown in Figure 2.

The above observations along with the known ionization energetics and biexciton photophysics allow a plausible overall reaction mechanism to be proposed. The essence of the proposed mechanism is that two-photon

excitation results in the TOP-ligated QD dissociating into a positively charged TOP ligand and a deligated, negatively charged QD, as indicated in reaction 1.

$$QD^{**}_{TOP} \xrightarrow{\text{Auger}} QD^{*}_{TOP}(h^*) \xrightarrow[\text{transfer}]{\text{charge}} QD^{-}/TOP^{+} \xrightarrow[\text{separation}]{\text{ion}} QD^{-}_{\text{unligated}} + TOP^{+}(\text{dark}) \quad \text{(reaction 1)}$$

The product QD has a greatly reduced luminescence QY for two different reasons. First, the loss of the TOP ligand leaves a surface trap state that acts as an electron−hole recombination center, and second, charged particles are typically only weakly luminescent. This is because when a negatively charged particle absorbs a photon it has two electrons and one hole. This negative "trion" undergoes comparatively fast nonradiative Auger decay, making the particle less luminescent than a neutral QD. This negatively charged state is often referred to as a "gray" state.[29,37−42] The PL recovers only when the TOP ligand is replaced and the charge neutralized. The difference in reaction probabilities for cadmium- versus selenium-rich particle surfaces can be understood in terms of reaction 1. Cadmium-rich surfaces will bind fewer TOP ligands[43] and therefore be less likely to undergo this reaction.

The separation of TOP^+ and QD^- ions occurring in chloroform, but not in octane, can be understood in terms of the energetics of charge separation. It is therefore useful to examine the biexciton photophysics which define the initial processes following two-photon excitation. Absorption of two photons produces a state at close to twice the (560 nm) bandgap energy, or 4.43 eV, as indicated in Scheme 1. Biexcitons (indicated as QD** in reaction 1) are known to undergo a fast Auger process in which the energy of one electron−hole pair is predominantly given to the other hole, exciting it to deep into the valence band.[28] The energetics of this excited hole state (indicated as *QD*(h*)* in reaction 1) are crucial to subsequent steps of the overall reaction and most easily considered in terms of ionization energies. The relevant energetics are shown in Scheme 1 and are obtained as follows: CdSe has a bulk valence band edge at about 5.8 eV below the vacuum level.[44] The quantum confinement energy for an exciton at 560 nm is about 0.47 eV, about 20% of which is in the hole. This puts the relaxed hole energy at about 5.9 eV. The energy of the lowest exciton is 2.21 eV, which can be put into either carrier by an Auger process. Auger transfer into the hole is the dominant process and puts the hot hole is at twice the bandgap energy, as depicted in Scheme 1. Thus, the hot hole at about 8.1 eV below the vacuum level. A realistic estimate of the errors involved in this determination is that it is likely correct to within 0.1 or 0.2 eV.

The TBP or TOP ionization energies do not appear to have been measured. However, the gas-phase triethylphosphine ionization energy has been determined by several different methods. It is reported to be anywhere between 7.6 and 8.52 eV by photoelectron spectroscopy[45,46] and 8.18 ± 0.05 by electron impact.[47] Vertical ionization energies are more relevant to an extremely fast charge transfer and are slightly higher, 8.3−8.4 eV.[48,49] The longer alkyl chains of TBP or TOP should lower the ionization energy very slightly. Using the vertical ionization energies, we conclude that two-photon hole ejection to form a separated QD^-/TOP^+ ion pair is approximately 0.2−0.3 eV energetically uphill (in vacuum) from the hot hole formed by the biexciton Auger process. Based on these energetics, one would conclude that the formation of gas phase separated ions should not occur. However, solvent stabilization plays a major role in the energetics of ion separation and can be estimated from electrostatic considerations, analogous to what is done in Marcus theory. An estimate for stabilization energy can be obtained by using a model in which reactants are treated as spheres of radii a_1 and a_2 and the solvent is treated as a dielectric continuum. The solvent stabilization energy is given by[50]

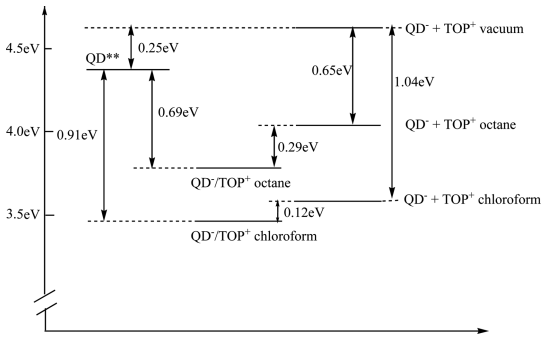

Scheme 1. State Energetics for 3.4 nm CdSe QDs

$$V = \frac{q}{4\pi\varepsilon_0}\left(\frac{1}{2a_1}+\frac{1}{2a_2}-\frac{1}{r}\right)\left(1-\frac{1}{\varepsilon}\right) \qquad (2)$$

where ε is its static dielectric constant, r is the distance between the centers of two reactants spheres and q is the electron charge. Evaluated for radii of 1.7 and 0.8 nm, for QD and a TOP molecule, respectively, solvent stabilization energies for (infinitely) separated QD^- and TOP^+ ions of 1.04 and 0.65 eV in chloroform ($\varepsilon = 4.8$) and octane (ε = 2.0), respectively, are obtained. Scheme 1 shows that separated ion-pair formation is energetically favorable in both solvents. However, formation of separated ions must occur through the contact ion pair, which is initially formed by hot hole transfer. The dissociation energies for a QD^-/TOP^+ contact ion pair is given by eq 3.

$$\Delta V_{sep} = \frac{q}{4\pi\varepsilon_0}\frac{1}{\varepsilon}\left(\frac{1}{a_1+a_2}\right) \qquad (3)$$

If we take the contact ion pair separation to be the sum of the ionic radii (0.8 and 1.7 nm), this simple calculation indicates that ion separation is energetically uphill by 0.12 eV in chloroform and 0.29 eV in

octane, as shown in Scheme 1. The contact ion pair can either separate or undergo charge recombination to return to the ground state. Charge recombination results in the luminescent particle being returned to its ground state—it has not lost ligands and is still bright. Thus, once the contact ion pair is formed, it is the competition between dissociation and charge recombination that determines the probability of photodarkening. These energetic considerations indicate that dissociation of the contact ion pair has a much higher Coulombic barrier in octane (0.29 eV) than in chloroform (0.12 eV), and this barrier causes the process of ion separation to not effectively compete with charge recombination in octane. The net result is a much lower photodarkening reaction probability in octane.

We have measured the reaction probabilities for several sizes of CdSe QDs varying from 2.8 to 4.6 nm in diameter. The results show little or no size dependence in the reaction probability over this range. For example, results on 4.6 nm particles show a slightly lower reaction probability, compared to the 3.4 nm particles. In this case, the observed reaction probability is about 0.04, which is about 30% lower than the 3.4 nm particles. The reaction probabilities are a sensitive function of the extent to which the particle surfaces are cadmium versus selenium rich, and the observed size dependent differences are probably within the batch-to-batch variability for each size. The lack of a strong size dependence can be understood in terms of two size dependent effects which change the reaction probability in opposite ways. First, the energetic driving force for charge transfer to form the contact ion pair decreases with increasing particle size. Since charge transfer competes with hot hole cooling, increasing particle size will tend to decrease the probability of forming the contact ion pair. Second, although dissociation of the contact ion pair is energetically unfavorable, it becomes less so as the particle size increases. Thus, once the contact ion pair is formed, the probability of forming the separated ion pair will increase with increasing particle size. The energetics associated with the formation and separation of the contact ion pair are shown in Scheme 1. Some quantitative aspects of the size dependent energetics of both processes can be considered. Scheme 1 shows that formation of the contact ion pair is very energetically favorable, about 0.91 eV for 3.4 nm CdSe particles. Hole cooling results in loss of 2.2 eV (the band gap energy) and charge transfer is energetically favorable only prior to the loss of 0.91 eV of this energy. Larger particles have less hole quantum confinement and a smaller bandgap energy and therefore produce a less energetic hot-hole state. Comparing 3.4 and 4.6 nm particles, the energetic difference between the hot-hole state and the contact ion pair state decreases from 0.91 to 0.59 eV. This smaller driving force would be expected to significantly decrease the probability of contact ion pair formation. The size-dependent energetics of contact ion pair separation go the other way. The separated ion pair is slightly energetically uphill, and the extent of this energetic barrier is given by eq 3. In the case of 4.6 nm particles in chloroform, the contact ion pair dissociation energy is calculated to be 23 meV less than for 3.4 particles, increasing the dissociation probability. We conclude that over this range of sizes these two effects approximately cancel each other and little size dependence of the photodarkening reaction probability is observed.

3. PL Recovery Kinetics. Recovery of the PL intensity requires that the negative charge on the QD be neutralized and that the newly-formed vacant surface site be passivated. The most simple and obvious mechanism for these two things to occur is through a concerted, second-order process in which a TOP^+ reattaches to a vacant surface site produced by TOP^+ dissociation. However, the PL recovery results in Figure 2 do not follow simple second-order kinetics. Furthermore, such a simple mechanism does not explain why the slow component closely matches the ligand addition and exchange kinetics in Figure 3. These observations suggest that the PL recovery mechanism is more complicated than a single, concerted reaction. We propose a mechanism in which charge recombination with TOP^+ is relatively fast and followed by ligation with either OAm, TOP, or $Cd(OA)_2$. This assignment makes sense in terms of the ion concentrations and the lack of charge-transfer steric considerations. Charge neutralization can occur whenever the TOP^+ comes in contact with a negatively charged QD, with little or no steric restriction. It seems reasonable that this reaction could occur at close to a diffusion limited rate. A simple calculation[51] shows that with this assumption and at the present concentrations charge neutralization should be very fast. The QD concentrations are typically 1−2 μM, and typically 25% of the particles undergo photodarkening. Thus, the initial QD^- and TOP^+ concentrations are on the order of 0.5 μM. If the TOP^+ hydrodynamic radius is taken to be 0.8 nm, then calculation of the diffusion limited second-order charge recombination rate constant for singly charged ions in chloroform gives a value of about 4.6×10^{10} L mol^{-1} s^{-1}. The overall time scale for charge recombination can be taken to be the initial half-life, and with the present concentrations, this is on the order of 20 μs. This is much faster than the observed tens of minutes time scale for PL recovery, and it follows that the rate of PL recovery is limited by subsequent ligand reactions. Religation could occur with either the TOP or OAm ligands in solution and could be followed ligand rearrangement or exchange. Although these ligand reactions could be fairly complicated the basic idea is that it is ligand reactions, rather than charge recombination that limits the PL recovery. A very simple version of this mechanism is indicated in Scheme 2.

The proposed mechanism starts with the charged, unligated QD (QD^-_x) and postulates two potential

intermediates: the neutral, unligated QD (QD_x) and the neutral QD, ligated with OAm (QD_A). The proposed mechanism also postulates four reaction rates: charge neutralization (k_N), ligation with TOP or OAm (k_P or k_A, respectively), and OAm to TOP ligand exchange (k_X). Reactions 2−5 correspond to the reactions indicated in parentheses in Scheme 2. The relatively fast charge recombination in this mechanism results in a significant simplification: the charged QD, ligated with OAm or TOP, are not considered. These species correspond to the "gray state" in blinking studies and are discussed later.

Passivation by $Cd(OA)_2$ can also be considered, and Figure 4 shows that the PL recovery kinetics depend on the concentration of cadmium oleate in solution. Without the addition of $Cd(OA)_2$, the PL recovery kinetics are dominated by a 120 min component. This is assigned to TOP and OAm passivation of the vacant site on the QD. Addition of $Cd(OA)_2$ results in a large 8.5 min recovery component, reaction 6 (Scheme 2). In Figure 4, TOP and OAm are present at concentrations of 15 and 20 mM, respectively. The concentration of added $Cd(OA)_2$ is about 0.65 mM, more than 1 order of magnitude lower than the TOP and OAm concentrations. These results indicate that $Cd(OA)_2$ more rapidly passivates the surface site vacated by the TOP^+ dissociation than does a solution-phase TOP ligand and that k_{Cd} is much larger than k_P or the smaller of k_A and k_X.

Although the relative rates in reactions 2−6 are qualitatively consistent with the observed reaction times, the biexponential recovery in Figure 4 indicates that this mechanism is somewhat oversimplified. Specifically, a fast reaction with excess $Cd(OA)_2$ should result in a single exponential decay, with the rate dominated by reaction 6 (Scheme 2). The presence of the slower, 120 min decay component indicates that not all of the TOP ligation sites are equally reactive with cadmium ions. The presence both fast and slow components indicates that some of the sites are reactive with TOP but essentially unreactive with $Cd(OA)_2$. This type of surface inhomogeneity is common and is why QD ensembles rarely give exponential PL kinetics.

Reactions 3−6 are pseudo-first-order processes, and as such the mechanism in Scheme 2 predicts that quantum dot concentration should have little effect on the PL recovery kinetics. Figure 5 shows that this is the case.

In this experiment, the irradiated sample was diluted by a factor of 1.8 immediately following irradiation. The diluent is a chloroform solution containing the same concentrations of TOP and OAm (60 and 40 mM, respectively) as the reaction solution. Thus, only the QD^- and TOP^+ concentrations are reduced. The resulting PL recovery curve is scaled by a factor of 1.8 for comparison to the undiluted sample; see Figure 5. The diluted and undiluted samples show comparable

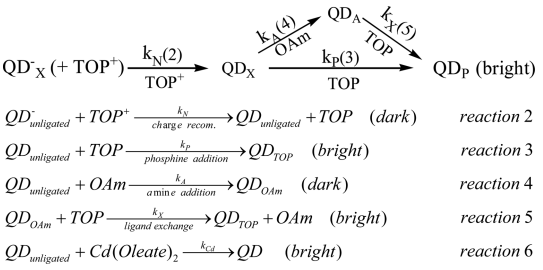

Scheme 2. Proposed Two-Photon Reaction Mechanism (Numbers in Parentheses Indicate the Reaction Numbers Shown Below the Mechanism)

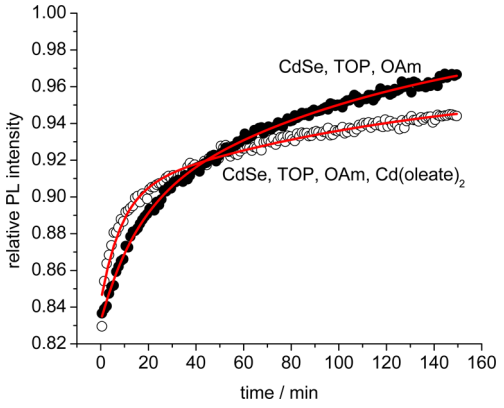

Figure 4. Plots of relative PL intensity as a function of recovery time for identical samples with (open circles) and without (solid circles) added cadmium oleate. Also shown are fit curves corresponding to an 120 min slow component and an 8.5 min (with $Cd(OA)_2$) and 14 min (without $Cd(OA)_2$) component.

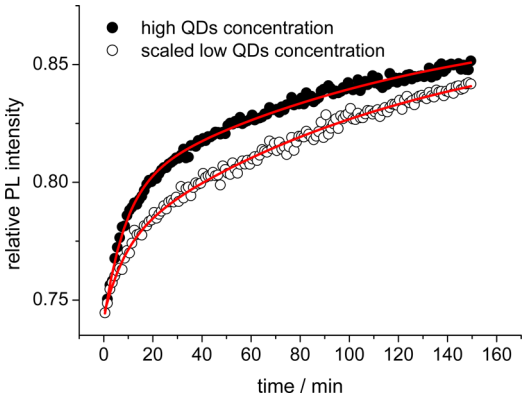

Figure 5. PL recovery kinetics as a function of QD concentration. The low concentrations results have been scaled by the dilution factor for comparison with the high concentration results. Also shown are fit curves having 8.5 and 120 min decay components. The 8.5 min components are 23% and 42% of the recoveries for the low and high concentrations, respectively.

amounts of PL recovery, and both recover on the same time scale, with both samples showing 8.5 and 120 min recovery components. This is consistent with the reactions in Scheme 2. Figure 5 also shows that the relative amplitude of the 8.5 min component in the undiluted sample is a factor of 1.8 larger than in the diluted sample.

We assign this component to the initial solution having a small but significant concentration of residual $Cd(OA)_2$ that comes through the purification process with the particles; see Figure 4. In the case of Figure 5, no $Cd(OA)_2$ has been added to either solution but the residual $Cd(OA)_2$ is sufficient to cause a significant fast recovery component. Dilution causes a factor of 1.8 drop in the concentration of residual $Cd(OA)_2$, resulting in the correspondingly smaller fast component for the diluted solution.

4. Charged Quantum Dots. One can also consider the possibility that ligand recombination (reactions 3−6) occurs on the same or faster time scale than charge neutralization (reaction 2). If this occurs, then a ligated, negatively charged QD would be formed. The extra electron could be in either the conduction band or localized in a surface trap state. If the electron were in the conduction band, then photoexcitation of this species would produce a negative "trion", a species having two conduction band electrons and a valence band hole. As mentioned above, such species have been postulated in the literature on quantum dot blinking. It has been suggested that Auger recombination competes with radiation, making the luminescence quantum yield of these species lower than that of the uncharged particles; they are assigned as being the "gray state" in blinking studies.[29,37−42] The presence of two conduction band electrons results in a radiative rate that is twice that of the single exciton. Thus, in the present experiments, the spectral signature of these charged particles should be a comparatively intense, short-lived component in PL decays. The magnitude of such a component would be expected to vary as PL recovery occurs. Literature reports indicate that negative trions have a lifetime on the order of 100−400 ps. Cohn *et al.*[22] report a negative trion lifetime of about 150 ps for this size of CdSe QD. Our studies of the positive trions and biexcitons suggest a negative trion time of about 350 ps for this size particle.[52] These times are comparable to or somewhat longer than the temporal response function of our TCSPC apparatus (about 150 ps), and we infer that if a high concentration of negative trions were being produced we should be able to detect them. PL decays are shown in Figure 6 and show no evidence of a fast component that could be assigned to charged QDs.

The primary difference in these decays is the amplitude, with little change in the kinetics. We have looked for the trions with several different sizes of particles with different types of surface ligands, but in all cases of these single-component CdSe QDs no indication of the trion is detected. The most obvious reason is that charge neutralization occurs very rapidly and a significant concentration of charged QDs does not build up in the solution (Scheme 2). This explanation is consistent with reported rates of QD charge neutralization.[24,53] It is also consistent with calculated diffusion limited charge

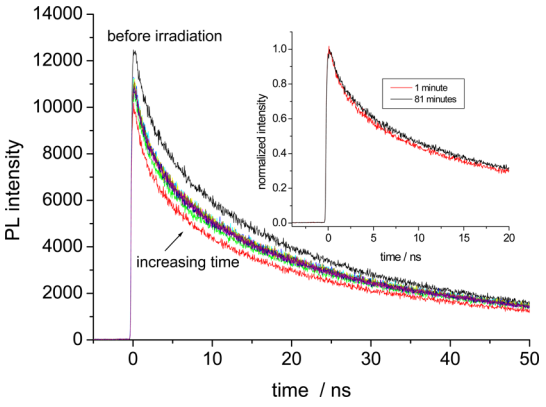

Figure 6. Time-resolved PL decay curves taken before irradiation and at increasing times after irradiation (1−81 min), as indicated. The inset shows normalized 1 and 81 min decays.

recombination rates discussed above and all of the other results presented here. All of this suggests that the charge recombination occurs much faster than ligand reattachment in these particles, as indicated in the mechanism in Scheme 2. We cannot, however completely rule out the possibility that charged QDs are present and the excess electron is in a surface trap. A surface-trapped electron could undergo rapid radiationless recombination with a hole produced by photoexcitation, rendering the particle dark. However, this seems unlikely because the PL quantum yield of these particles is moderately high (typically 20−30%), and one would expect a significant fraction of the charged particles to have the excess electron in the conduction band.

CONCLUSIONS

In this paper, we have systematically studied the two-photon chemistry of CdSe QDs. The conclusions of these studies may be summarized as follows.

(1) Upon intense irradiation, CdSe quantum dots undergo two-photon excitation to produce a biexciton, which ultimately results in a loss of photoluminescence quantum yield, photodarkening. We have established that upon absorption of two or more photons the quantum yield for this process is on the order of 3−6% in chloroform and much smaller in nonpolar solvents, such as octane.

(2) An analysis of the energetics and solvent dependence of the photodarkening reaction indicates that following two-photon excitation the biexciton undergoes an Auger process that produces a hot hole. The hot hole may relax or be ejected to a surface-bound TOP ligand, forming a QD^-/TOP^+ contact ion pair. The ion pair dissociates to separated ions in chloroform, but not in octane.

(3) The photodarkening reaction may or may not be reversible, depending on whether an excess of surface ligands is present in the irradiated solution.

Concentration-dependent studies indicate that charge recombination occurs rapidly, followed by ligand reattachment and reorganization on a longer (tens of minutes) time scale.

(4) The negatively charged quantum dot is not observed in the spectroscopic measurements. This is presumably because of the fast charge recombination mechanism.

Finally, we note that although the photodarkening mechanism elucidated here is studied in the context of two-photon excitation, it is probably much more general. The mechanism is based on the production of a hot hole by an Auger process. We have recently shown that neutral CdSe/CdS and CdSe/ZnSe core/shell QDs undergo thermally induced surface charging.[52,54] This results in a particle having a surface-bound electron and a hole in the valence band. Photoexcitation results in two valence band holes and a conduction band electron—it is essentially a positive trion. This species can also undergo an Auger process, producing a hot hole which could do exactly the same chemistry as is described here. As such, the mechanism described here could be a significant one-photon photodegradation mechanism for CdSe-based QDs. The extent to which this occurs is currently being studied and will be reported in later papers.

EXPERIMENTAL SECTION

Chemicals. Cadmium oxide (CdO, 99.5%), trioctylphosphine oxide (TOPO, 90%), octadecylamine (ODA, 90%), trioctylphosphine (TOP, 97%), octadecene (ODE, 90%), oleylamine (OAm, 70%), and hexane (99.8%) were obtained from Aldrich. Selenium (Se, 99%), oleic acid (OA, 90%), and chloroform ($CHCl_3$, 99.8%) were obtained from Alfa Aesar. ODA were recrystallized from toluene before use. TOPO was purified by repeated recrystallization from acetonitrile. Chloroform and acetone were purified by distillation over P_2O_5. Oleylamine was purified by vacuum distillation over calcium hydride. All other chemicals were used without further purification.

Synthesis of 2.8 nm CdSe Particles. CdO (0.2 mmol, 25.7 mg) was mixed with 300 mg of steric acid and 2.5 mL of ODE and heated to 250 °C to obtain a colorless solution under N_2 flow. After the solution was cooled to room temperature, 1.0 g of ODA and 0.4 g of TOPO were added. The mixture was then heated to 275 °C. At this temperature, a selenium solution containing 1 mmol (78 mg) of Se, 0.90 g (2.4 mmol, 1.1 mL) of trioctylphosphine (TOP), and 0.7 mL of ODE was quickly injected under N_2. The heating mantle was removed immediately after the injection, and the reaction was quenched after 20−30s.

Synthesis of 3.4 nm CdSe Particles. CdO (0.2 mmol, 25.7 mg) was mixed with 0.4 mL of oleic acid, and 2.5 mL ODE and was heated to 250 °C to obtain a colorless solution under N_2 flow. After the solution was cooled to room temperature, 1.0 g of ODA and 0.4 g of TOPO were added. The mixture was then heated to 280 °C. At this temperature, a selenium solution containing 1 mmol (78 mg) of Se, 0.90 g (2.4 mmol, 1.1 mL) of trioctylphosphine (TOP), and 0.7 mL of ODE was quickly injected under N_2. The reaction was kept at 255−260 °C for 1−2 min and then cooled to room temperature.

Synthesis of 4.6 nm CdSe Particles. CdO (0.2 mmol, 25.7 mg) was mixed with 0.4 mL of oleic acid and 2.5 mL of ODE and was heated to 250 °C to obtain a colorless solution under N_2 flow. The Se precursor was prepared by dissolving 1 mmol (78 mg) of Se into a mixture of 1 mL of TBP and 0.7 mL of ODE at 200 °C. When the whole mixture was cooled to room temperature, 0.5 mL of oleylamine was added. The Se precursor was injected into the Cd precursor at 285 °C, and the reaction was then maintained at 250 °C for 2.5 min.

Purification Method. In a typical purification, 1 mL of as-synthesized CdSe solution was added to 2 mL of acetone and the mixture centrifuged followed by removal of the supernatant. Hexane (3 mL) was then added to dissolve the precipitated particles. The solution was cooled in the ice bath and centrifuged for several minutes to remove undissolved solids. The hexane supernatant was decanted along with the dissolved particles and acetone added to reprecipitate the particles from solution. The supernatant was removed, and the particles were resuspended in chloroform-based solutions containing different amounts of TOP, OAm, and $Cd(OA)_2$ for spectroscopic measurements. The amounts of TOP, OAm, and $Cd(OA)_2$ were measured using a 50 μL glass syringe to give the concentrations specified in the text.

Characterization. UV−vis spectra were taken using a Cary 50 SCAN UV−vis spectrophotometer. Static photoluminescence measurements were performed using a Jobin-Yvon Fluorolog-3 spectrometer. The instrument consists of a xenon lamp/double monochromator excitation source and a spectrograph/CCD detector. Time-resolved luminescence measurements were conducted by time-correlated single-photon counting (TCSPC), exciting samples with very low intensity 410 nm pulses at 1 MHz from a cavity-dumped frequency-doubled Coherent MIRA laser. In all cases, the luminescence was focused through a 0.25m monochromator with a 150 groove/mm grating onto a Micro Photon Devices PDM 50CT SPAD detector.

Measurement of Luminescence Quantum Yields. Quantum yields were determined by comparison of the nanoparticle spectra with the spectrum of dilute Rhodamine 6G (R6G) in methanol using the appropriate spectral calibration factors. This comparison involves collection of the luminescence spectra in face-on geometry. The absorbance of the nanoparticles and Rhodamine 6G samples were small, typically about 0.1. The quantum yields are determined by taking the ratio of areas under the luminescence spectra. These spectra are corrected for monochromator throughput and detector efficiency. The nanoparticles and Rhodamine 6G PL spectra are at close to the same wavelengths, so the relative correction factors are close to unity. The quantum yield of nanoparticles is calculated by

$$\Phi_{\text{particle}} = \frac{1 - 10^{-A_{\text{R6G}}}}{1 - 10^{-A_{\text{particle}}}} \frac{S_{\text{particle}}}{S_{\text{R6G}}} \times \Phi_{\text{R6G}}$$

where A_{R6G} and A_{particle} are the absorbance of R6G and nanoparticles at excitation wavelength, respectively, S_{R6G} and S_{particle} are the corrected areas under the fluorescence curves of R6G and nanoparticles, respectively, and Φ_{R6G} is the quantum yield of R6G in the dilute methanol solution, taken to be 95%.

Samples Irradiation. Sample excitation is accomplished with the 387.5 nm second harmonic of a Clark CPA 2001 light source, which produces 140 fs, 600 μJ, 775 nm pulses at a repetition of 1 kHz. Sample excitation is with the second harmonic of this light, at 387 nm. The excitation power at the sample was typically 8 mW and focused to a beam diameter of about 1.3 mm for an irradiation time of 15 to 60 s. The power-dependent experiments were done at somewhat higher powers (18.5 mW) for shorter times (10 s).

Conflict of Interest: The authors declare no competing financial interest.

Acknowledgment. This material is based upon work supported by the U.S. Department of Energy, Office of Science, Office of Basic Energy Sciences, under Award No. DE-FG02-13ER16371.

REFERENCES AND NOTES

1. Manna, L.; Scher, E. C.; Li, L.; Alivisatos, A. P. Epitaxial Growth and Photochemical Annealing of Graded CdS/ZnS Shells on Colloidal CdSe Nanorods. *J. Am. Chem. Soc.* **2002**, *124*, 7136–7145.
2. Jones, M.; Nedeljkovic, J.; Ellingson, R. J.; Nozik, A. J.; Rumbles, G. Photoenhancement of Luminescence in Colloidal CdSe Quantum Dot Solutions. *J. Phys. Chem. B* **2003**, *107*, 11346–11352.
3. Shimizu, K. T.; Woo, W. K.; Fisher, B. R.; Eisler, H. J.; Bawendi, M. G. Surface-Enhanced Emission from Single Semiconductor Nanocrystals. *Phys. Rev. Lett.* **2002**, *89*, 117401.
4. Hess, B. C.; Okhrimenko, I. G.; Davis, R. C.; Stevens, B. C.; Schulzke, Q. A.; Wright, K. C.; Bass, C. D.; Evans, C. D.; Summers, S. L. Surface Transformation and Photoinduced Recovery in CdSe Nanocrystals. *Phys. Rev. Lett.* **2001**, *86*, 3132–3135.
5. Wang, Y.; Tang, Z.; Correa-Duarte, M. A.; Pastoriza-Santos, I.; Giersig, M.; Kotov, N. A.; Liz-Marzán, L. M. Mechanism of Strong Luminescence Photoactivation of Citrate-Stabilized Water-Soluble Nanoparticles with CdSe Cores. *J. Phys. Chem. B* **2004**, *108*, 15461–15469.
6. Asami, H.; Abe, Y.; Ohtsu, T.; Kamiya, I.; Hara, M. Surface State Analysis of Photobrightening in CdSe Nanocrystal Thin Films. *J. Phys. Chem. B* **2003**, *107*, 12566–12568.
7. Osborne, M. A.; Lee, S. F. Quantum Dot Photoluminescence Activation and Decay: Dark, Bright, and Reversible Populations in ZnS-Capped CdSe Nanocrystals. *ACS Nano* **2011**, *5*, 8295–8304.
8. Chon, J. W. M.; Zijlstra, P.; Gu, M.; van Embden, J.; Mulvaney, P. Two-Photon-Induced Photoenhancement of Densely Packed CdSe/ZnSe/ZnS Nanocrystal Solids and its Application to Multilayer Ooptical Data Storage. *Appl. Phys. Lett.* **2004**, *85*, 5514–5516.
9. Uematsu, T.; Maenosono, S.; Yamaguchi, Y. Photoinduced Fluorescence Enhancement in Mono- and Multilayer Films of CdSe/ZnS Quantum Dots: Dependence on Intensity and Wavelength of Excitation Light. *J. Phys. Chem. B* **2005**, *109*, 8613–8618.
10. Wu, F.; Lewis, J. W.; Kliger, D. S.; Zhang, J. Z. Unusual Excitation Intensity Dependence of Fluorescence of CdTe Nanoparticles. *J. Chem. Phys.* **2003**, *118*, 12–16.
11. Rodríguez-Viejo, J.; Mattoussi, H.; Heine, J. R.; Kuno, M. K.; Michel, J.; Bawendi, M. G.; Jensen, K. F. Evidence of Photo- and Electrodarkening of (CdSe)ZnS Quantum Dot Composites. *J. Appl. Phys.* **2000**, *87*, 8526–8534.
12. Nirmal, M.; Dabbousi, B. O.; Bawendi, M. G.; Macklin, J. J.; Trautman, J. K.; Harris, T. D.; Brus, L. E. Fluorescence Intermittency in Single Cadmium Selenide Nanocrystals. *Nature* **1996**, *383*, 802.
13. Banin, U.; Bruchez, M.; Alivisatos, A. P.; Ha, T.; Weiss, S.; Chemla, D. S. Evidence for a Thermal Contribution to Emission Intermittency in Single CdSe/CdS Core/Shell Nanocrystals. *J. Chem. Phys.* **1999**, *110*, 1195–1201.
14. Efros, A. L.; Rosen, M. Random Telegraph Signal in the Photoluminescence Intensity of a Single Quantum Dot. *Phys. Rev. Lett.* **1997**, *78*, 1110.
15. Chepic, D. I.; Efros, A. L.; Ekimov, A. I.; Ivanov, M. G.; Kharchenko, V. A.; Kudriavtsev, I. A.; Yazeva, T. V. Auger Ionization of Semiconductor Quantum Drops in a Glass Matrix. *J. Lumin.* **1990**, *47*, 113–127.
16. Krauss, T. D.; Brus, L. E. Charge, Polarizability, and Photoionization of Single Semiconductor Nanocrystals. *Phys. Rev. Lett.* **1999**, *83*, 4840–4843.
17. Padilha, L. A.; Robel, I.; Lee, D. C.; Nagpal, P.; Pietryga, J. M.; Klimov, V. I. Spectral Dependence of Nanocrystal Photoionization Probability: The Role of Hot-Carrier Transfer. *ACS Nano* **2011**, *5*, 5045–5055.
18. Wang, H.; de Mello Donegá, C.; Meijerink, A.; Glasbeek, M. Ultrafast Exciton Dynamics in CdSe Quantum Dots Studied from Bleaching Recovery and Fluorescence Transients. *J. Phys. Chem. B* **2006**, *110*, 733–737.
19. Lenngren, N.; Garting, T.; Zheng, K.; Abdellah, M.; Lascoux, N.; Ma, F.; Yartsev, A.; Žídek, K.; Pullerits, T. Multiexciton Absorption Cross Sections of CdSe Quantum Dots Determined by Ultrafast Spectroscopy. *J. Phys. Chem. Lett.* **2013**, *4*, 3330–3336.
20. Shabaev, A.; Efros, A. L.; Nozik, A. J. Multiexciton Generation by a Single Photon in Nanocrystals. *Nano Lett.* **2006**, *6*, 2856–2863.
21. Zhu, H.; Song, N.; Rodríguez-Córdoba, W.; Lian, T. Wave Function Engineering for Efficient Extraction of up to Nineteen Electrons from One CdSe/CdS Quasi-Type II Quantum Dot. *J. Am. Chem. Soc.* **2012**, *134*, 4250–4257.
22. Cohn, A. W.; Rinehart, J. D.; Schimpf, A. M.; Weaver, A. L.; Gamelin, D. R. Size Dependence of Negative Trion Auger Recombination in Photodoped CdSe Nanocrystals. *Nano Lett.* **2014**, *14*, 353–358.
23. McGuire, J. A.; Sykora, M.; Joo, J.; Pietryga, J. M.; Klimov, V. I. Apparent *versus* True Carrier Multiplication Yields in Semiconductor Nanocrystals. *Nano Lett.* **2010**, *10*, 2049.
24. McGuire, J. A.; Sykora, M.; Robel, I.; Padilha, L. A.; Joo, J.; Pietryga, J. M.; Klimov, V. I. Spectroscopic Signatures of Photocharging due to Hot-Carrier Transfer in Solutions of Semiconductor Nanocrystals under Low-Intensity Ultraviolet Excitation. *ACS Nano* **2010**, *4*, 6087.
25. Wu, K.; Zhu, H.; Lian, T. Ultrafast Exciton Dynamics and Light-Driven H2 Evolution in Colloidal Semiconductor Nanorods and Pt-Tipped Nanorods. *Acc. Chem. Res.* **2015**, *48*, 851–859.
26. Yang, Y.; Lian, T. Multiple Exciton Dissociation and Hot Electron Extraction by Ultrafast Interfacial Electron Transfer from PbS QDs. *Coord. Chem. Rev.* **2014**, *263-264*, 229–238.
27. Jiang, Z.-J.; Kelley, D. F. Hot and Relaxed Electron Transfer from CdSe Core and Core/Shell Nanorods. *J. Phys. Chem. C* **2011**, *115*, 4594–4602.
28. Park, Y.-S.; Bae, W. K.; Pietryga, J. M.; Klimov, V. I. Auger Recombination of Biexcitons and Negative and Positive Trions in Individual Quantum Dots. *ACS Nano* **2014**, *8*, 7288–7296.
29. Jha, P. P.; Guyot-Sionnest, P. Trion Decay in Colloidal Quantum Dots. *ACS Nano* **2009**, *3*, 1011–1015.
30. Gong, K.; Zeng, Y.; Kelley, D. F. Extinction Coefficients, Oscillator Strengths, and Radiative Lifetimes of CdSe, CdTe, and CdTe/CdSe Nanocrystals. *J. Phys. Chem. C* **2013**, *117*, 20268–20279.
31. Scott, R.; Achtstein, A. W.; Prudnikau, A.; Antanovich, A.; Christodoulou, S.; Moreels, I.; Artemyev, M.; Woggon, U. Two Photon Absorption in II–VI Semiconductors: The Influence of Dimensionality and Size. *Nano Lett.* **2015**, *15*, 4985–4992.
32. Makarov, N. S.; Lau, P. C.; Olson, C.; Velizhanin, K. A.; Solntsev, K. M.; Kieu, K.; Kilina, S.; Tretiak, S.; Norwood, R. A.; Peyghambarian, N.; Perry, J. W. Two-Photon Absorption in CdSe Colloidal Quantum Dots Compared to Organic Molecules. *ACS Nano* **2014**, *8*, 12572–12586.
33. Jasieniak, J.; Smith, L.; van Embden, J.; Mulvaney, P.; Califano, M. Re-examination of the Size-Dependent Absorption Properties of CdSe Quantum Dots. *J. Phys. Chem. C* **2009**, *113*, 19468–19474.
34. Karel Capek, R. K.; Moreels, I.; Lambert, K.; De Muynck, D.; Zhao, Q.; Van Tomme, A.; Vanhaecke, F.; Hens, Z. Optical Properties of Zincblende Cadmium Selenide Quantum Dots. *J. Phys. Chem. C* **2010**, *114*, 6371–6376.
35. Van Stryland, E. W.; Vanherzeele, H.; Woodall, M. A.; Soileau, M. J.; Smirl, A. L.; Guha, S.; Boggess, T. F. Two Photon Absorption, Nonlinear Refraction, and Optical Limiting in Semiconductors. *Opt. Eng.* **1985**, *24*, 613.
36. Sheik-Bahae, M.; Said, A. A.; Wei, T.; Hagan, D. J.; Van Stryland, E. W. Sensitive Measurement of Optical Nonlinearities Using a Single Beam. *IEEE J. Quantum Electron.* **1990**, *26*, 760.
37. Manceau, M.; Vezzoli, S.; Glorieux, Q.; Pisanello, F.; Giacobino, E.; Carbone, L.; De Vittorio, M.; Bramati, A. Effect of Charging on CdSe/CdS Dot-in-Rods Single-Photon Emission. *Phys. Rev. B: Condens. Matter Mater. Phys.* **2014**, *90*, 035311–35319.
38. Qin, W.; Liu, H.; Guyot-Sionnest, P. Small Bright Charged Colloidal Quantum Dots. *ACS Nano* **2014**, *8*, 283–291.

39. Qin, W.; Shah, R. A.; Guyot-Sionnest, P. CdSeS/ZnS Alloyed Nanocrystal Lifetime and Blinking Studies under Electrochemical Control. *ACS Nano* **2012**, *6*, 912–918.
40. Galland, C.; Ghosh, Y.; Steinbruck, A.; Sykora, M.; Hollingsworth, J. A.; Klimov, V. I.; Htoon, H. Two Types of Luminescence Blinking Revealed by Spectroelectrochemistry of Single Quantum Dots. *Nature* **2011**, *479*, 203–207.
41. Galland, C.; Ghosh, Y.; Steinbrück, A.; Hollingsworth, J. A.; Htoon, H.; Klimov, V. I. Lifetime Blinking in Nonblinking Nanocrystal Quantum Dots. *Nat. Commun.* **2012**, *3*, 908–914.
42. Gómez, D. E.; van Embden, J.; Mulvaney, P.; Fernée, M. J.; Rubinsztein-Dunlop, H. Exciton−Trion Transitions in Single CdSe-CdS Core-Shell Nanocrystals. *ACS Nano* **2009**, *3*, 2281–2287.
43. Kim, W.; Lim, S. J.; Jung, S.; Shin, S. K. Binary Amine-Phosphine Passivation of Surface Traps on CdSe Nanocrystals. *J. Phys. Chem. C* **2010**, *114*, 1539–1546.
44. West, A. R. *Basic Solid State Chemistry*; Wiley: Chichester, 1988.
45. Yarbrough, L. W., II; Hall, M. B. Photoelectron Spectra of Substituted Chromium, Molybdenum, and Tungsten Pentacarbonyls. Relative π-Acceptor and σ-Donor Properties of Various Phosphorus Ligands. *Inorg. Chem.* **1978**, *17*, 2269.
46. Aue, D. H.; Bowers, M. T., Stabilities of Positive Ions From Equilibrium Gas Phase Bbasicity Measurements. In *Ions Chemistry*; Bowers, M. T., Ed.; Elsevier, 1979; p 1.
47. Distefano, G.; Innorta, G.; Pignataro, S.; Foffani, A. Correlation Between the Ionization Potentials of Transition Metal Complexes and of the Corresponding Ligands. *J. Organomet. Chem.* **1968**, *14*, 165.
48. Weiner, M. A.; Lattman, M. Ultraviolet Photoelectron Spectra of Some Cr(CO)5L Complexes Containing Organosulfide and Organophosphine Ligands. *Inorg. Chem.* **1978**, *17*, 1084.
49. Cowley, A. H.; Goodman, D. W.; Kuebler, N. A.; Sanchez, M.; Verkade, J. G. Molecular Photoelectron Spectroscopic Investigation of Some Caged Phosphorus Compounds and Related Acyclic Species. *Inorg. Chem.* **1977**, *16*, 854.
50. Kelley, A. M. *Condensed-Phase Molecular Spectroscopy and Photophysics*; Wiley: Hoboken, NJ, 2013.
51. Steinfeld, J. I.; Francisco, J. S.; Hase, W. L. *Chemical Kinetics and Dynamics*, 2nd ed.; Prentice Hall: Upper Saddle River, NJ, 1999.
52. Gong, K.; Kelley, D. F. Surface Charging and Trion Dynamics in CdSe-Based Core/Shell Quantum Dots. *J. Phys. Chem. C* **2015**, *119*, 9637–9645.
53. Midgett, A. G.; Hillhouse, H. W.; Hughes, B. K.; Nozik, A. J.; Beard, M. C. Flowing *versus* Static Conditions for Measuring Multiple Exciton Generation in PbSe Quantum Dots. *J. Phys. Chem. C* **2010**, *114*, 17486–17500.
54. Cai, X.; Martin, J. E.; Shea-Rohwer, L. E.; Gong, K.; Kelley, D. F. Thermal Quenching Mechanisms in II-VI Semiconductor Nanocrystals. *J. Phys. Chem. C* **2013**, *117*, 7902–7913.